Title

Antitumor Activity of 1,18-Octadecanedioic Acid-Paclitaxel Complexed with Human Serum Albumin.

Journal

Journal of the American Chemical Society, 141(30)

ISSN

0002-7863

Authors

Callmann, Cassandra E
LeGuyader, Clare LM
Burton, Spencer T
et al.

Publication Date

2019-07-01

DOI

10.1021/jacs.9b04272

Peer reviewed

JACS JOURNAL OF THE AMERICAN CHEMICAL SOCIETY

Communication

Cite This: J. Am. Chem. Soc. 2019, 141, 11765−11769

pubs.acs.org/JACS

Antitumor Activity of 1,18-Octadecanedioic Acid-Paclitaxel Complexed with Human Serum Albumin

Cassandra E. Callmann,[†,‡] Clare L. M. LeGuyader,[†] Spencer T. Burton,[‡] Matthew P. Thompson,[†,‡] Robert Hennis,[†] Christopher Barback,[§] Niel M. Henriksen,[∥] Warren C. Chan,[†] Matt J. Jaremko,[†] Jin Yang,[∥] Arnold Garcia,[∥] Michael D. Burkart,[†] Michael K. Gilson,[∥] Jeremiah D. Momper,[∥] Paul A. Bertin,[#] and Nathan C. Gianneschi*[,†,‡]

[†]Department of Chemistry & Biochemistry, University of California San Diego, La Jolla, California 92093, United States

[‡]Departments of Chemistry, Materials Science & Engineering, Biomedical Engineering, Chemistry of Life Processes Institute, International Institute for Nanotechnology, Simpson Querrey Institute, Northwestern University, Evanston, Illinois 60208, United States

[§]Department of Radiology, University of California San Diego, La Jolla, California 92093, United States

[∥]Skaggs School of Pharmacy and Pharmaceutical Sciences, University of California San Diego, La Jolla, California 92093, United States

[#]Elevance Renewable Sciences, Inc. 2501 Davey Road, Woodridge, Illinois 60517, United States

Supporting Information

ABSTRACT: We describe the design, synthesis, and antitumor activity of an 18 carbon α,ω-dicarboxylic acid monoconjugated via an ester linkage to paclitaxel (PTX). This 1,18-octadecanedioic acid-PTX (**ODDA-PTX**) prodrug readily forms a noncovalent complex with human serum albumin (HSA). Preservation of the terminal carboxylic acid moiety on **ODDA-PTX** enables binding to HSA in the same manner as native long-chain fatty acids (LCFAs), within hydrophobic pockets, maintaining favorable electrostatic contacts between the ω-carboxylate of **ODDA-PTX** and positively charged amino acid residues of the protein. This carrier strategy for small molecule drugs is based on naturally evolved interactions between LCFAs and HSA, demonstrated here for PTX. **ODDA-PTX** shows differentiated pharmacokinetics, higher maximum tolerated doses and increased efficacy *in vivo* in multiple subcutaneous murine xenograft models of human cancer, as compared to two FDA-approved clinical formulations, Cremophor EL-formulated paclitaxel (crPTX) and Abraxane (nanoparticle albumin-bound (nab)-paclitaxel).

Harnessing human serum albumin (HSA) as a drug carrier in oncology is an established strategy aimed to improve dosing, safety, and efficacy.[1−4] HSA is the most abundant serum protein with myriad functions, including a central role in metabolic pathways as a transporter of long-chain fatty acids (LCFAs) and hydrophobic molecules, both natural and synthetic.[5−7] Recently, HSA and its endogenous ligands have gained interest for their roles in dysregulated metabolism tied to tumor growth.[8,9] HSA is scavenged by solid tumors as a catabolic source of glutamine.[10,11] Further, exogenous LCFA uptake and metabolism are prominent in the metastatic progression of human cancers with poor prognoses,[12−15] as sustained tumor growth requires upregulation of nutrient acquisition. Therefore, drug-modified LCFAs that mimic the natural binding modes with HSA is a drug delivery strategy for cancer with potential in optimized dosing, stability, solubility, and efficacy by hitchhiking on these metabolic pathways.

Binding interactions between HSA and LCFAs have been extensively studied, with as many as 7 moderate- to high-affinity binding pockets identified through nuclear magnetic resonance (NMR) and protein crystallography.[16−19] In five of these sites, LCFA binding is stabilized through specific electrostatic interactions between the terminal LCFA carboxylate anion and positively charged amino acid residues at the base of otherwise hydrophobic binding pockets of HSA. These interactions are a consistent structural feature of thermodynamically stable, natural binding modes between LCFAs and HSA. However, in classical drug lipidation strategies, this electrostatic interaction is extinguished when the single carboxylic acid of an LCFA is conjugated to the warhead, often via ester, amide, or hydrazone linkage.[20−25] Indeed, the first and only example utilizing a long-chain fatty diacid, Ozempic (semaglutide), was approved by the FDA in 2017. Maintaining the naturally evolved LCFA carboxylate contact is a critical feature contributing to semaglutide's performance as a once-weekly glucagon-like-peptide-1 receptor agonist for type-2 diabetes.[26]

Herein, we employ an 18 carbon α,ω-dicarboxylic acid as the HSA-binding motif of a prodrug conjugate. This conserves the high affinity electrostatic interactions between the ω-carboxylate and HSA, while maintaining the α-carboxylate for drug conjugation. This approach preserves the natural binding mode and mimics HSA engagement of natural LCFAs (Figure 1). Specifically, 1,18-octadecanedioic acid (ODDA) was conjugated to paclitaxel (PTX) to produce a mono-

Received: April 19, 2019
Published: July 18, 2019

DOI: 10.1021/jacs.9b04272
J. Am. Chem. Soc. 2019, 141, 11765−11769

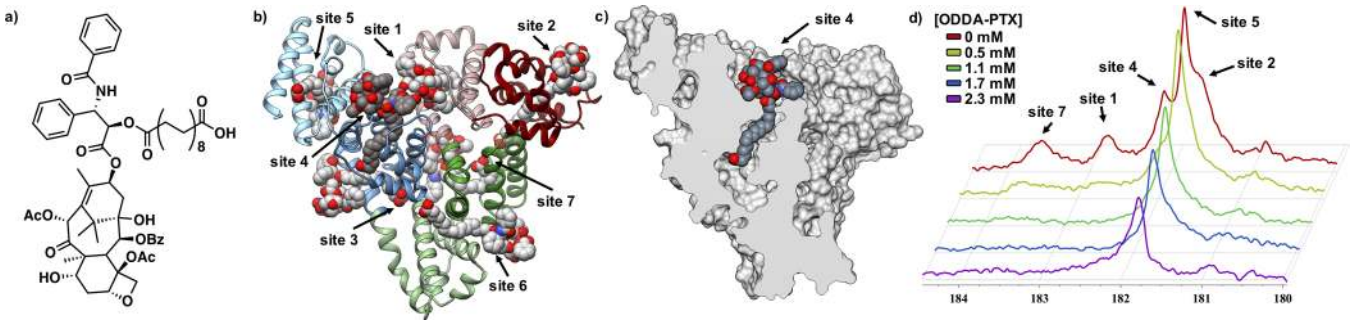

Figure 1. Design of **ODDA-PTX** and HSA binding. (a) Chemical structure of **ODDA-PTX**. (b) Modeling of **ODDA-PTX** binding to 7 LCFA sites on HSA. (c) Molecular model of HSA with **ODDA-PTX** bound in native LCFA site 4 (sphere). (d) NMR titration of **ODDA-PTX** into a pre-equilibrated, saturated solution of palmitic-1-^{13}C acid (C16:0, 2.3 mM) with HSA (0.45 mM). **ODDA-PTX** displaces C16:0 in all observable fatty acid binding pockets at concentrations lower than that of the native ligand, demonstrating a high binding affinity to HSA.

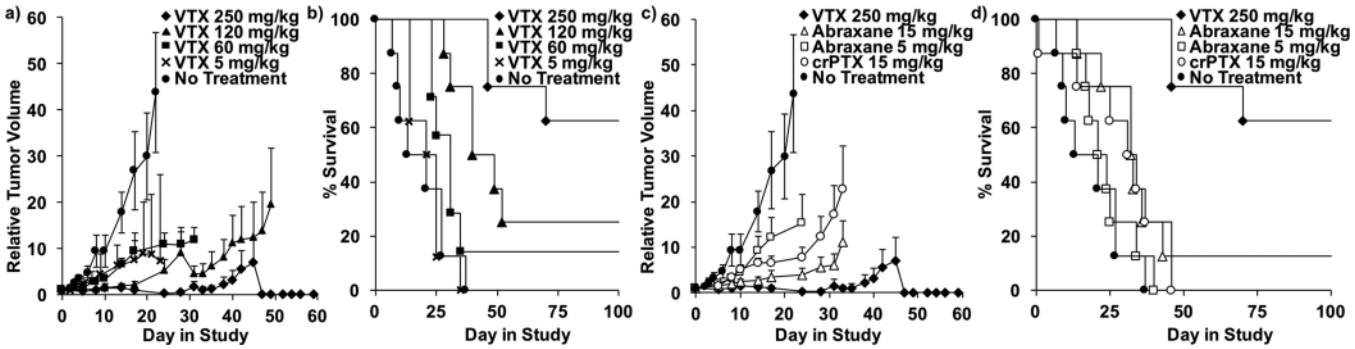

Figure 2. Efficacy and survival in HT-1080 fibrosarcoma model (n = 8 per group). Doses were administered IV via tail vein (q7dx4). (a) Dose–response of **VTX** with respect to PTX concentration, as compared to nontreated animals. Tumor volume is relative to initial volume on first day of treatment. Efficacy graphs for each group are truncated once survival drops below 50%. (b) Corresponding survival plot to panel a. (c) Relative tumor growth for **VTX** versus Abraxane and crPTX at MTD. (d) Corresponding survival plot to panel c. In this model, doses of Abraxane could not exceed 15 mg/kg due to toxicity (see SI).

functionalized PTX ester at the 2′-hydroxyl (**ODDA-PTX**, Figure 1a, Figures S1 and S2). PTX is one of the most widely used chemotherapeutic agents. PTX promotes tubulin polymerization and arrests cell division, leading to apoptotic cell death.[27] Functionalization of PTX at the 2′-hydroxyl prevents this mode of action.[28] Indeed, an *in vitro* polymerization assay confirmed **ODDA-PTX** performed as a prodrug (Figure S3). Therefore, cytotoxic activity of **ODDA-PTX** is regained only when PTX is free from ODDA.

ODDA-PTX was mixed with HSA to yield a water-soluble complex at a 5:1 prodrug:protein mol ratio, designated **VTX** (Figure 1b,c. "V" = Roman numeral for five, signifying the number of equivalents of **ODDA-PTX** per HSA. "TX" = taxane). **VTX** was readily reconstituted in PBS following lyophilization, yielding a homogeneous solution. HSA binding sites for palmitic acid (C16:0) and other LCFAs are known;[16,17] thus the interaction of **ODDA-PTX** with HSA was examined experimentally by NMR displacement studies[18,19] with palmitic-1-^{13}C acid (Figure 1d). **ODDA-PTX** was titrated into a pre-equilibrated solution of HSA with palmitic-1-^{13}C acid, showing its rapid displacement.

To corroborate these data, **VTX** was modeled using molecular dynamics simulations (Figure 1b,c, Figures S4–S6, Table S1). It was determined that fatty acid binding sites 1, 2, 4, and 5 were the most likely binding locations for **ODDA-PTX**; modes consistent with native binding of LCFAs. Importantly, **VTX** preserves the tertiary structure and thermal stability of HSA as determined by circular dichroism spectroscopy (Figure S7). A rapid equilibrium dialysis assay showed that >95% of **ODDA-PTX** was bound to HSA down to 0.5 μM (Table S2), with isothermal titration calorimetry confirming multiple binding sites (Figure S8). Dynamic light scattering and cryogenic transmission electron microscopy revealed **VTX** as a fully dispersed prodrug:protein complex, similar to native HSA, not a nanoparticulate aggregate (Figure S9).

The cell-free stability of **ODDA-PTX** and **VTX** was assayed over a range of conditions by high performance liquid chromatography (Figures S10–S12). Cytotoxicity of **VTX** was assessed *in vitro*, confirming activity at nM concentrations with respect to PTX (Table S3). The metabolic stability and *in vitro* intrinsic clearance of **ODDA-PTX** was compared to PTX in human liver microsomes (Figure S13), demonstrating similar rates of metabolism. Significantly, blocking the fatty acid translocase/CD36 receptor, a key protein involved in uptake of LCFAs across cell membranes[29] with implications in metastatic cancers,[15,30] reduced the cytotoxicity of **ODDA-PTX**, but not PTX (Figure S14). This provides evidence that **ODDA-PTX** enters cells through different pathways from PTX, and importantly, through the same pathways as LCFAs.

VTX was evaluated as an antitumor agent in subcutaneous xenograft mouse models of human cancer. Therapeutic efficacy was determined by monitoring tumor growth and survival versus nontreated controls and compared to two FDA-approved paclitaxel formulations, Abraxane (nanoparticle albumin-bound PTX) and Cremophor-formulated PTX

DOI: 10.1021/jacs.9b04272
J. Am. Chem. Soc. 2019, 141, 11765–11769

Table 1. Calculated PK Parameteres of Paclitaxel Released from VTX and Abraxane Following Single IV Injection in HT-1080 Murine Xenografts[a,b]

Group	C_{max} (ng/mL)	AUC ((h·ng)/mL)	V_{dist} (mL)	$t_{1/2}$ (h)
VTX	508 ± 188	4688 ± 797	1257 ± 374	9.80 ± 1.20
Abraxane	1607 ± 469	5640 ± 469	481 ± 163	4.39 ± 0.62

[a]Animals dosed at 20 mg/kg with respect to paclitaxel content of each formulation. [b]Detected entity is intact paclitaxel.

(crPTX). Initial studies were carried out in the HT-1080 human fibrosarcoma model, as it is predictable, fast-growing, and known to be taxane-responsive (Figure 2).[31,32] The therapeutic index (TI) was defined as the ratio of maximum tolerated dose (MTD) to minimum effective dose (MED),[33] where MTD was the highest nonlethal deliverable dose and less than 20% weight loss,[34] and MED was the lowest dose showing a delay in tumor growth relative to nontreated controls.[35] Efficacy of **VTX** was investigated in the HT-1080 model following intravenous (IV) injection at 5, 60, 120, and 250 mg/kg with respect to PTX concentration every 7 days for 4 weeks (q7dx4). Animals responded to **VTX** in a dose-dependent manner (Figure 2a). Complete tumor regression (5/8) or dramatically suppressed progression was observed in animals administered **VTX** at 250 mg/kg, with no evidence of drug-associated toxicity observed (Figure 2b, Figures S15 and S16). Conversely, animals administered Abraxane at 20 mg/kg with respect to PTX concentration experienced significant treatment-associated lethality (Figure S17). Therefore, the highest dose of Abraxane administered in this model was limited to 15 mg/kg. We note that these MTDs are lower than what is reported in several published studies.[36−38] Similar antitumor activity of crPTX at 15 mg/kg was observed to that of Abraxane at 15 mg/kg (Figure 2c,d), the reported MTD of crPTX.[39]

Elevated doses of **VTX** significantly extended survival time and inhibited tumor growth over nontreated controls (Figure 2b and Figure S18), whereas the improvement of survival time for Abraxane and crPTX was modest. The lowest administered dose (5 mg/kg) of **VTX** and Abraxane had similar effects on median survival time and both treatments sufficiently suppressed tumor growth relative to nontreated controls over the course of the study (p-value = 0.041 and 0.045, respectively, based on an unpaired t test where $p < 0.05$ was considered statistically significant). This was defined as the MED for both **VTX** and Abraxane in this model and with this dosing regimen (Figure S19). In evaluating the efficacy in tumor growth suppression and survival of animals treated with **VTX** and Abraxane, we conclude a distinct advantage of **VTX** over the FDA-approved drug. In this model, **VTX** had a MED of 5 mg/kg and a MTD of >250 mg/kg with respect to PTX concentration. Higher doses could not be explored due to solubility constraints of HSA used in the formulation of **VTX**. Thus, the TI of **VTX** is >50 in the HT-1080 model at a q7dx4 dosing regimen. Conversely, Abraxane-treated animals experienced significant toxicity at all doses exceeding 15 mg/kg (see Figure S17), revealing a TI of 3 for Abraxane.

Pharmacokinetic (PK) parameters of **VTX** and Abraxane were determined in both healthy and tumor-burdened (HT-1080 xenograft) nu/nu mice and calculated using standard noncompartmental methods (Table 1).[40] At 1 h postinjection, both the metabolite PTX and **ODDA-PTX** were found in plasma samples from animals administered **VTX**. However, **ODDA-PTX** is present at a 5-fold higher concentration than PTX. Maximum plasma concentration (C_{max}) of PTX in animals administered Abraxane at 20 mg/kg is similar to those administered **VTX** at 250 mg/kg (Figures S20 and S21). Half-life and area under the plasma concentration versus time curve (AUC) of PTX in animals treated with **VTX** is higher than that of Abraxane, suggesting that **VTX** acts as a drug depot for the cytotoxin.

Biodistribution of **VTX** dosed at 250 mg/kg with respect to PTX content in HT-1080 xenografts was evaluated in comparison to Abraxane and crPTX in both the tumor and the liver at 1, 4, and 24 h postinjection (Figure 3). The highest

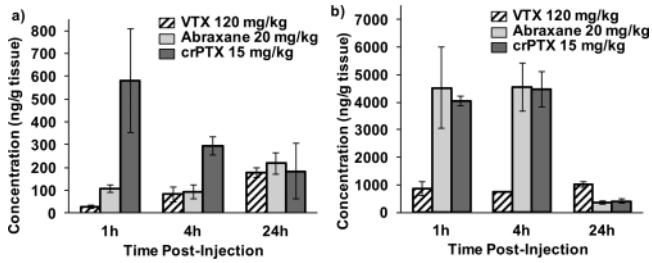

Figure 3. Biodistribution of PTX (n = 3 per group). Concentration of PTX in HT-1080 xenografts at 1, 4, and 24 h postinjection with either **VTX**, Abraxane, or crPTX in (a) tumor and (b) liver.

initial tumor concentration was in animals administered crPTX (Figure 3a). However, the tumor concentration of metabolite PTX in animals administered **VTX** steadily increased as a function of time, consistent with the depot-like PK data. Minimal accumulation in the liver was observed for **VTX**, compared to the high levels observed for both the nanoscale aggregates of Abraxane (see Figure S9) and crPTX at early time points (Figure 3b). It has been proposed that Cremophor imparts nanoparticle-like properties to the crPTX formulation[41] with liver accumulation as a result.

Given the promising efficacy and tolerance (as measured by body weight) observed at 250 mg/kg with respect to PTX concentration, the toxicity of **VTX** at this dose in nu/nu mice was further evaluated following IV injection (q7dx4) and compared to crPTX and Abraxane at 15 mg/kg. A complete blood count (CBC) panel and serum chemical analysis was obtained 24 h after the final injection (Table S4, Figures S22 and S23). Nearly all parameters were equivalent between all treatment groups, despite animals being administered **VTX** at a 16-fold higher dose of PTX than those administered Abraxane or crPTX (Figures S24 and S25).

Additional efficacy studies were completed in HT-29 (human colorectal adenocarcinoma)[3] and PANC-1 (human pancreas ductal carcinoma) models, both known targets of taxane therapy (Figure 4).[3,42] The trends in efficacy from the HT-1080 model were also observed in these models, where **VTX** at 250 mg/kg was well-tolerated and flat-lined tumor growth (Figure 4, Figure S26). Abraxane showed no significant therapeutic effect at 15 mg/kg in the PANC-1 model. Thus, we explored Abraxane at a higher dose (30 mg/kg) with 2/8 mice experiencing acute lethality (Figure S27). Conversely, 2

DOI: 10.1021/jacs.9b04272
J. Am. Chem. Soc. 2019, 141, 11765−11769

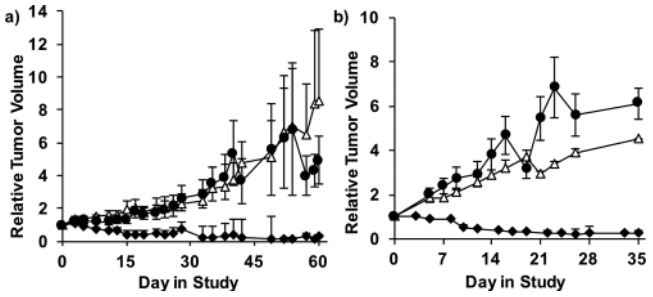

Figure 4. Efficacy of VTX (n = 8 per group) in xenograft models. (a) Pancreatic carcinoma PANC-1, and (b) colorectal adenocarcinoma HT-29.

animals experienced complete tumor regression upon administration of high doses of **VTX**.

In conclusion, we have developed a carrier system for albumin-mediated delivery of PTX. The design strategy is based on mimicking the natural interaction between HSA and LCFAs, by monofunctionalizing ODDA with PTX. We have demonstrated efficacy of **VTX** in three xenograft models: HT-1080 (fibrosarcoma), PANC-1 (pancreatic cancer), and HT-29 (colon cancer). The overall survival of animals is significantly extended when administered **VTX**, compared to clinical formulations. The PK profile of **VTX** differs significantly from Abraxane, as does the biodistribution compared to Abraxane and crPTX. Given the relationship between HSA, fatty acids, and the tumor microenvironment, this is a potential strategy for drug delivery to cancers that have increased demands for HSA and fatty acids.[43,44] This may be of importance in cancers that demonstrate multidrug resistance, where conventional PTX treatment is ineffective.[45,46] We propose this strategy as a generalizable new route for the facile modification of drugs for engaging HSA without the need for complex nanoscale formulations or covalent modification of the protein.[47]

■ ASSOCIATED CONTENT

Supporting Information

The Supporting Information is available free of charge on the ACS Publications website at DOI: 10.1021/jacs.9b04272.

Synthetic schemes, statistical analyses, methods, molecular dynamics simulations details (PDF)

Amber files (ZIP)

■ AUTHOR INFORMATION

Corresponding Author

*nathan.gianneschi@northwestern.edu

ORCID

Niel M. Henriksen: 0000-0002-7916-0757

Michael D. Burkart: 0000-0002-4472-2254

Michael K. Gilson: 0000-0002-3375-1738

Nathan C. Gianneschi: 0000-0001-9945-5475

Notes

The authors declare the following competing financial interest(s): N.C.G. acknowledges a conflict of interest as a founder and shareholder of Vybyl Biopharma, Inc., a licensee of related technologies. M.K.G. has an equity interest in and is a cofounder and scientific advisor of VeraChem LLC.

■ ACKNOWLEDGMENTS

Research was conducted with support from Elevance Renewable Sciences. C.E.C. thanks both the ARCS Foundation and the Inamori Foundation for fellowship support. W.C.C. and M.J.J. were supported by NIH/NCI T32 CA009523. The authors thank Dr. Yongxuan Su and the UC San Diego Mass Spectrometry Facility for assistance with LC/MS. The authors also thank Dr. Irawati Kandela and the Developmental Therapeutics Core at Northwestern University, as well as Dr. Jianjun Wei at Northwestern University, for assistance with toxicity and pathology analyses.

■ REFERENCES

(1) Hoogenboezem, E. N.; Duvall, C. L. Harnessing albumin as a carrier for cancer therapies. *Adv. Drug Delivery Rev.* **2018**, *130*, 73−89.

(2) Elsadek, B.; Kratz, F. Impact of albumin on drug delivery–new applications on the horizon. *J. Controlled Release* **2012**, *157* (1), 4−28.

(3) Desai, N.; Trieu, V.; Yao, Z.; Louie, L.; Ci, S.; Yang, A.; Tao, C.; De, T.; Beals, B.; Dykes, D.; Noker, P.; Yao, R.; Labao, E.; Hawkins, M.; Soon-Shiong, P. Increased antitumor activity, intratumor paclitaxel concentrations, and endothelial cell transport of cremophor-free, albumin-bound paclitaxel, ABI-007, compared with cremophor-based paclitaxel. *Clin. Cancer Res.* **2006**, *12* (4), 1317−24.

(4) Shan, L.; Zhuo, X.; Zhang, F.; Dai, Y.; Zhu, G.; Yung, B. C.; Fan, W.; Zhai, K.; Jacobson, O.; Kiesewetter, D. O.; Ma, Y.; Gao, G.; Chen, X. A paclitaxel prodrug with bifunctional folate and albumin binding moieties for both passive and active targeted cancer therapy. *Theranostics* **2018**, *8* (7), 2018−2030.

(5) Kragh-Hansen, U. Structure and ligand binding properties of human serum albumin. *Danish Med. Bull.* **1990**, *37* (1), 57−84.

(6) Ghuman, J.; Zunszain, P. A.; Petitpas, I.; Bhattacharya, A. A.; Otagiri, M.; Curry, S. Structural basis of the drug-binding specificity of human serum albumin. *J. Mol. Biol.* **2005**, *353* (1), 38−52.

(7) van der Vusse, G. J. Albumin as fatty acid transporter. *Drug Metab. Pharmacokinet.* **2009**, *24* (4), 300−7.

(8) Michalopoulou, E.; Bulusu, V.; Kamphorst, J. J. Metabolic scavenging by cancer cells: when the going gets tough, the tough keep eating. *Br. J. Cancer* **2016**, *115*, 635.

(9) Merlot, A. M.; Kalinowski, D. S.; Richardson, D. R. Unraveling the mysteries of serum albumin—more than just a serum protein. *Front. Physiol.* **2014**, *5*, 299.

(10) White, E. Exploiting the bad eating habits of Ras-driven cancers. *Genes Dev.* **2013**, *27* (19), 2065−2071.

(11) Commisso, C.; Davidson, S. M.; Soydaner-Azeloglu, R. G.; Parker, S. J.; Kamphorst, J. J.; Hackett, S.; Grabocka, E.; Nofal, M.; Drebin, J. A.; Thompson, C. B.; Rabinowitz, J. D.; Metallo, C. M.; Vander Heiden, M. G.; Bar-Sagi, D. Macropinocytosis of protein is an amino acid supply route in Ras-transformed cells. *Nature* **2013**, *497*, 633.

(12) Carracedo, A.; Cantley, L. C.; Pandolfi, P. P. Cancer metabolism: fatty acid oxidation in the limelight. *Nat. Rev. Cancer* **2013**, *13* (4), 227−32.

(13) Hirschey, M. D.; DeBerardinis, R. J.; Diehl, A. M. E.; Drew, J. E.; Frezza, C.; Green, M. F.; Jones, L. W.; Ko, Y. H.; Le, A.; Lea, M. A.; Locasale, J. W.; Longo, V. D.; Lyssiotis, C. A.; McDonnell, E.; Mehrmohamadi, M.; Michelotti, G.; Muralidhar, V.; Murphy, M. P.; Pedersen, P. L.; Poore, B.; Raffaghello, L.; Rathmell, J. C.; Sivanand, S.; Vander Heiden, M. G.; Wellen, K. E. Dysregulated metabolism contributes to oncogenesis. *Sem. Cancer Biol.* **2015**, *35*, S129−S150.

(14) Vander Heiden, M. G.; Cantley, L. C.; Thompson, C. B. Understanding the Warburg Effect: The Metabolic Requirements of Cell Proliferation. *Science* **2009**, *324* (5930), 1029−1033.

(15) Pascual, G.; Avgustinova, A.; Mejetta, S.; Martín, M.; Castellanos, A.; Attolini, C. S.-O.; Berenguer, A.; Prats, N.; Toll, A.; Hueto, J. A.; Bescós, C.; Di Croce, L.; Benitah, S. A. Targeting metastasis-initiating cells through the fatty acid receptor CD36. *Nature* **2017**, *541*, 41.

(16) Curry, S.; Brick, P.; Franks, N. P. Fatty acid binding to human serum albumin: new insights from crystallographic studies. *Biochim. Biophys. Acta, Mol. Cell Biol. Lipids* **1999**, *1441* (2−3), 131−40.
(17) Curry, S.; Mandelkow, H.; Brick, P.; Franks, N. Crystal structure of human serum albumin complexed with fatty acid reveals an asymmetric distribution of binding sites. *Nat. Struct. Biol.* **1998**, *5* (9), 827−35.
(18) Simard, J. R.; Zunszain, P. A.; Ha, C. E.; Yang, J. S.; Bhagavan, N. V.; Petitpas, I.; Curry, S.; Hamilton, J. A. Locating high-affinity fatty acid-binding sites on albumin by x-ray crystallography and NMR spectroscopy. *Proc. Natl. Acad. Sci. U. S. A.* **2005**, *102* (50), 17958−17963.
(19) Simard, J. R.; Zunszain, P. A.; Hamilton, J. A.; Curry, S. Location of high and low affinity fatty acid binding sites on human serum albumin revealed by NMR drug-competition analysis. *J. Mol. Biol.* **2006**, *361* (2), 336−51.
(20) Bradley, M. O.; Swindell, C. S.; Anthony, F. H.; Witman, P. A.; Devanesan, P.; Webb, N. L.; Baker, S. D.; Wolff, A. C.; Donehower, R. C. Tumor targeting by conjugation of DHA to paclitaxel. *J. Controlled Release* **2001**, *74* (1), 233−236.
(21) Spector, A. A.; John, K.; Fletcher, J. E. Binding of long-chain fatty acids to bovine serum albumin. *J. Lipid Res.* **1969**, *10* (1), 56−67.
(22) Irby, D.; Du, C.; Li, F. Lipid−Drug Conjugate for Enhancing Drug Delivery. *Mol. Pharmaceutics* **2017**, *14* (5), 1325−1338.
(23) Sarett, S. M.; Werfel, T. A.; Lee, L.; Jackson, M. A.; Kilchrist, K. V.; Brantley-Sieders, D.; Duvall, C. L. Lipophilic siRNA targets albumin in situ and promotes bioavailability, tumor penetration, and carrier-free gene silencing. *Proc. Natl. Acad. Sci. U. S. A.* **2017**, *114* (32), E6490−e6497.
(24) Liu, H.; Moynihan, K. D.; Zheng, Y.; Szeto, G. L.; Li, A. V.; Huang, B.; Van Egeren, D. S.; Park, C.; Irvine, D. J. Structure-based Programming of Lymph Node Targeting in Molecular Vaccines. *Nature* **2014**, *507* (7493), 519−522.
(25) Liu, Z.; Chen, X. Simple bioconjugate chemistry serves great clinical advances: albumin as a versatile platform for diagnosis and precision therapy. *Chem. Soc. Rev.* **2016**, *45* (5), 1432−1456.
(26) Lau, J.; Bloch, P.; Schäffer, L.; Pettersson, I.; Spetzler, J.; Kofoed, J.; Madsen, K.; Knudsen, L. B.; McGuire, J.; Steensgaard, D. B.; Strauss, H. M.; Gram, D. X.; Knudsen, S. M.; Nielsen, F. S.; Thygesen, P.; Reedtz-Runge, S.; Kruse, T. Discovery of the Once-Weekly Glucagon-Like Peptide-1 (GLP-1) Analogue Semaglutide. *J. Med. Chem.* **2015**, *58* (18), 7370−7380.
(27) Wang, T.-H.; Wang, H.-S.; Soong, Y.-K. Paclitaxel-induced cell death. *Cancer* **2000**, *88* (11), 2619−2628.
(28) Sharma, S.; Lagisetti, C.; Poliks, B.; Coates, R. M.; Kingston, D. G. I.; Bane, S. Dissecting the Paclitaxel-Microtubule Association: Quantitative Assessment of the 2′-OH Group. *Biochemistry* **2013**, *52* (13), 2328−2336.
(29) Bonen, A.; Campbell, S. E.; Benton, C. R.; Chabowski, A.; Coort, S. L. M.; Han, X.-X.; Koonen, D. P. Y.; Glatz, J. F. C.; Luiken, J. J. F. P. Regulation of fatty acid transport by fatty acid translocase/CD36. *Proc. Nutr. Soc.* **2004**, *63* (2), 245−249.
(30) Liang, Y.; Han, H.; Liu, L.; Duan, Y.; Yang, X.; Ma, C.; Zhu, Y.; Han, J.; Li, X.; Chen, Y. CD36 plays a critical role in proliferation, migration and tamoxifen-inhibited growth of ER-positive breast cancer cells. *Oncogenesis* **2018**, *7* (12), 98.
(31) Vanhoefer, U.; Cao, S.; Harstrick, A.; Seeber, S.; Rustum, Y. M. Comparative antitumor efficacy of docetaxel and paclitaxel in nude mice bearing human tumor xenografts that overexpress the multidrug resistance protein (MRP). *Annals of oncology: official journal of the European Society for Medical Oncology* **1997**, *8* (12), 1221−8.
(32) Callmann, C. E.; Barback, C. V.; Thompson, M. P.; Hall, D. J.; Mattrey, R. F.; Gianneschi, N. C. Therapeutic Enzyme-Responsive Nanoparticles for Targeted Delivery and Accumulation in Tumors. *Adv. Mater.* **2015**, *27* (31), 4611−4615.
(33) Muller, P. Y.; Milton, M. N. The determination and interpretation of the therapeutic index in drug development. *Nat. Rev. Drug Discovery* **2012**, *11* (10), 751−761.
(34) Connett, J. M.; Buettner, T. L.; Anderson, C. J. Maximum tolerated dose and large tumor radioimmunotherapy studies of 64Cu-labeled monoclonal antibody 1A3 in a colon cancer model. *Clin. Cancer Res.* **1999**, *5* (10 Suppl), 3207s−3212s.
(35) Mach, C. M.; Mathew, L.; Mosley, S. A.; Kurzrock, R.; Smith, J. A. Determination of minimum effective dose and optimal dosing schedule for liposomal curcumin in a xenograft human pancreatic cancer model. *Anticancer Res.* **2009**, *29* (6), 1895−1899.
(36) Desai, N. P.; Trieu, V.; Hwang, L. Y.; Wu, R.; Soon-Shiong, P.; Gradishar, W. J. Improved effectiveness of nanoparticle albumin-bound (nab) paclitaxel versus polysorbate-based docetaxel in multiple xenografts as a function of HER2 and SPARC status. *Anti-Cancer Drugs* **2008**, *19* (9), 899−909.
(37) Miele, E.; Spinelli, G. P.; Tomao, F.; Tomao, S. Albumin-bound formulation of paclitaxel (Abraxane(®) ABI-007) in the treatment of breast cancer. *Int. J. Nanomed.* **2009**, *4*, 99−105.
(38) Zhao, M.; Lei, C.; Yang, Y.; Bu, X.; Ma, H.; Gong, H.; Liu, J.; Fang, X.; Hu, Z.; Fang, Q. Abraxane, the Nanoparticle Formulation of Paclitaxel Can Induce Drug Resistance by Up-Regulation of P-gp. *PLoS One* **2015**, *10* (7), No. e0131429.
(39) Huang, G. S.; Lopez-Barcons, L.; Freeze, B. S.; Smith, A. B.; Goldberg, G. L.; Horwitz, S. B.; McDaid, H. M. Potentiation of Taxol Efficacy by Discodermolide in Ovarian Carcinoma Xenograft-Bearing Mice. *Clin. Cancer Res.* **2006**, *12* (1), 298−304.
(40) Gabrielsson, J.; Weiner, D. Non-compartmental analysis. *Methods Mol. Biol. (N. Y., NY, U. S.)* **2012**, *929*, 377−89.
(41) Gelderblom, H.; Verweij, J.; Nooter, K.; Sparreboom, A. Cremophor EL: the drawbacks and advantages of vehicle selection for drug formulation. *Eur. J. Cancer* **2001**, *37* (13), 1590−8.
(42) Chiorean, E. G.; Von Hoff, D. D. Taxanes: impact on pancreatic cancer. *Anti-Cancer Drugs* **2014**, *25* (5), 584−92.
(43) Kamphorst, J. J.; Nofal, M.; Commisso, C.; Hackett, S. R.; Lu, W.; Grabocka, E.; Vander Heiden, M. G.; Miller, G.; Drebin, J. A.; Bar-Sagi, D.; Thompson, C. B.; Rabinowitz, J. D. Human pancreatic cancer tumors are nutrient poor and tumor cells actively scavenge extracellular protein. *Cancer Res.* **2015**, *75* (3), 544−53.
(44) Liu, Q.; Luo, Q.; Halim, A.; Song, G. Targeting lipid metabolism of cancer cells: A promising therapeutic strategy for cancer. *Cancer Lett.* **2017**, *401*, 39−45.
(45) Gottesman, M. M.; Fojo, T.; Bates, S. E. Multidrug resistance in cancer: role of ATP−dependent transporters. *Nat. Rev. Cancer* **2002**, *2*, 48.
(46) Podolski-Renić, A.; Anđelković, T.; Banković, J.; Tanić, N.; Ruždijić, S.; Pešić, M. The role of paclitaxel in the development and treatment of multidrug resistant cancer cell lines. *Biomed. Pharmacother.* **2011**, *65* (5), 345−353.
(47) Kratz, F.; Warnecke, A.; Scheuermann, K.; Stockmar, C.; Schwab, J.; Lazar, P.; Druckes, P.; Esser, N.; Drevs, J.; Rognan, D.; Bissantz, C.; Hinderling, C.; Folkers, G.; Fichtner, I.; Unger, C. Probing the cysteine-34 position of endogenous serum albumin with thiol-binding doxorubicin derivatives. Improved efficacy of an acid-sensitive doxorubicin derivative with specific albumin-binding properties compared to that of the parent compound. *J. Med. Chem.* **2002**, *45* (25), 5523−33.

DOI: 10.1021/jacs.9b04272
J. Am. Chem. Soc. 2019, 141, 11765−11769